Title

Structural transition of nanogel star polymers with pH by controlling PEGMA interactions with acid or base copolymers

Journal

Molecular Physics, 114(21)

ISSN

0026-8976

Authors

Felberg, LE
Doshi, A
Hura, GL
et al.

Publication Date

2016-11-01

DOI

10.1080/00268976.2016.1224942

Peer reviewed

Structural Transition of Nanogel Star Polymers with pH by Controlling PEGMA Interactions with Acid or Base Copolymers

Lisa E. Felberg[1†], Anjali Doshi[2†], Greg L. Hura[5], Joseph Sly[6], Victoria A. Piunova[6], William C. Swope[6], Julia E. Rice[6], Robert Miller[6], Teresa Head-Gordon[1-5*]

[1]Department of Chemical and Biomolecular Engineering, [2]Department of Bioengineering, [3]Department of Chemistry, University of California, Berkeley, California 94720, USA

[4]Chemical Sciences Division and [5]Physical Biosciences Division, Lawrence Berkeley National Labs, Berkeley, California 94720, USA

[6]IBM Research, IBM Almaden Research Center, San Jose, California 95120, USA

We use small angle x-ray scattering (SAXS) to characterize a class of star diblock polymers with a nanogel core on which the outer block arms are comprised of random co-polymers of temperature sensitive PEGMA with pH sensitive basic (PDMAEMA) and acidic (PMAA) monomers. The acquired SAXS data shows that many of the nanogel star polymers undergo a sharp structural transition over a narrow range of pH, but with unexpectedly large shifts in the apparent pKa with respect to that of the acidic or basic monomer unit, the linear polymer form, or even an alternate star polymer with a tightly cross-linked core chemistry. We have demonstrated a distinct and quantifiable structural response for the nanogel star copolymers by altering the core or by pairing the monomers PDMAEMA-PEGMA and PMAA-PEGMA to achieve structural transitions that have typically been observed in stars through changes in arm length and number.

*corresponding author, thg@berkeley.edu.

† Both authors contributed equally to work presented here.

INTRODUCTION

The use of nanoparticle delivery vehicles such as liposomes[1], dendrimers[2], micelles[3], and star polymers[4-6] offer great promise for medical applications that require in vivo delivery of functional materials such as pharmaceuticals and imaging agents[7,8]. Of specific importance to biomedical applications is the development and characterization of poly(ethylene glycol) (PEG) nanoparticles, since their high water solubility, thermo-sensitivity, and low immunogenicity have made it the most recognized polymer chemistry exhibiting biocompatibility and increased circulation time in vivo.[1-3,9-11] Although PEG-based polymers have been widely used in biomedical applications, there are known limitations in its synthetic functionalization, for example to create sensitivity to pH changes. Smart polymers that exhibit a pH induced structural response are important since different tissue environments and cell compartments exhibit a wide variation in pH, and thus offer the potential for a more targeted delivery of therapeutic drugs[8,12].

Recently, the use of non-metal organocatalysis for ring opening polymerization has allowed for great ease in synthesis of novel nanogel star polymers, in which polymer “arms” are connected to a cross-linked polymer core[13,14], with high uniformity (polydispersity indices <1.1) and with the ability to control for size (15 – 40 nm)[15-17]. Given this early promise there is nonetheless a large unexplored chemical landscape of possible star polymers of varied size and chemical composition which require characterization under physiological conditions of aqueous solvent, and how they respond to relevant stimuli such as temperature, pH, and buffers.

Here we present a systematic Small Angle X-ray Scattering (SAXS) study to characterize a series of polyelectrolyte star polymers composed of a divinylbenzene (DVB) crosslinked nanogel core, and diblock copolymer arms consisting of a hydrophobic block of poly-styrene (PS) followed by a hydrophilic block of (1) neutral poly(ethylene glycol) methacrylate (PEGMA): DVB-PS-PEGMA, (2) acidic poly(methacrylic acid) (PMAA): DVB-PS-PMAA, (3) basic poly(2-dimethylaminoethyl methacrylate) (PDMAEMA): DVB-PS-PDMAEMA, (4) 50% PMAA and 50% PEGMA distributed randomly in the outer block: DVB-PS-$PMAA_{50\%}$/$PEGMA_{50\%}$, and (5) 50% PDMAEMA and 50% PEGMA distributed randomly in the outer block: DVB-PS-$PDMAEMA_{50\%}$/$PEGMA_{50\%}$,. While there are a number of studies on the behavior of linear and weak polyelectrolyte star polymers, they have been largely confined to homopolymers and have focused on a thermal response and the position of the LCST.[18]

While the DVB-PS-PEGMA and the DVB-PS-PMAA star polymers do not undergo structural transitions over the evaluated pH range, we show that the DVB-PS-PMAA$_{50\%}$/PEGMA$_{50\%}$, DVB-PS-PDMAEMA$_{50\%}$/PEGMA$_{50\%}$, and DVB-PS-PDMAEMA star polymers undergo a sharp structural transition over a narrow range of pH, consistent with their titration curves, but with unexpectedly large shifts in the apparent pKa when compared to the linear polymer form or even a star polymer with a more tightly cross-linked core. Our studies provide a molecular level understanding for pairing of PEGMA with acidic and basic substituents, and the effect of pH, on copolymer nanogel star architectures. This work illustrates the ability to fine-tune a structural transition response to desired pH through control of chemical composition of the arms and nanogel star polymer architecture.

EXPERIMENTAL METHODS

***General procedures*:** ^{1}H NMR spectra were obtained on a Bruker Avance 2000 spectrometer (^{1}H, 400 MHz)**,** and were referenced to internal solvent residue (CDCl3: ^{1}H = 7.26 ppm). All NMR spectra were recorded at ambient temperature using standard Bruker library pulse programs and are reported as the fully proton-decoupled spectra. Analytical Gel Permeation Chromatography (GPC) using Waters high resolution columns HR1, HR2, HR4E and HR5E (flow rate 1 mL / min, THF) in conjunction with a waters 996 photodiode array and/or a waters 411 differential refractometer was used to determine molecular weight distributions, Mw/Mn, of polymer samples with respect to linear polystyrene standards. Light Scattering measurements were made to determine Mw, Mw/Mn, using the aforementioned column set with a Wyatt DAWN EOS multi-angle light-scattering detector, QELS quasi elastic light scattering detector and Optilab (intraferometric refractometer). Deuterated solvents were purchased from Cambridge Isotopes, Inc. and used as received. 3-(tert-Butyldimethylsilyloxy)-1-propyl lithium (20 wt% solution in cyclohexane) was purchased from FMC Lithium Division and used as received. Styrene (S), 2-(dimethylamino)ethyl methacrylate (DMAEMA), tert-butyl methacrylate (tBuMA) and N,N,N′,N″,N″-Pentamethyldiethylenetriamine (PMDETA) were purchased from Sigma-Aldrich and purified by vacuum distillation over CaH_2. Poly(ethylene glycol) methyl ether methacrylate (PEGMA) was also obtained from Sigma-Aldrich and purified by passing through basic alumina column. Para-divinylbenzene (p-DVB), Cu(I)Cl and dry solvents were purchased from Sigma-Aldrich and used as received.

Synthesis of DVB-PS-PDMAEMA. Nanogel core Polystyrene star macroinitiators and Poly (N,N-dimethylaminoethyl methacrylate)-b-Polystyrene Star Polymer (PS-PDMAEMA Star) were synthesized as reported earlier.[19]

Synthesis of DVB-PS-PEGMA. ATRP-macroinitiator nanogel star polymer (2.0 g, Mn arm = 2.8 kDa, 35 arms), PEGMA (34.3g) and PMDETA (0.12g) were dissolved in anisole (65 mL). Three freeze-pump-thaw cycles were performed and then Cu(I)Cl (0.07g) was added under positive Ar flow. The reaction mixture was sealed under Ar atmosphere before being heated to 45° C. After 60 min, the reaction mixture was cooled down in liquid N_2, opened to air and precipitated into hexanes twice. Obtained white gooey solid was freeze-dried from dioxane. Yield: 18% (6.5 g). ^{1}H NMR (400 MHz, $CDCl_3$, δ) = 7.27-6.30 (br. m, 135 H), 4.5-4.05 (br. s, 41H), 4.05-3.45 (br. m, 383H), 3.45-3.05 (br. s, 62H), 2.20-1.55 (br. s, 28H), 1.55-0.9 (br. m, 95H), DLS (THF): Mw = 315 kDa (1.37), DP (PEGMA) = 20 (6.1 kDa)

Synthesis of DVB-PS-PMAA. ATRP-macroinitiator nanogel star polymer (0.27 g, Mn arm = 3.7 kDa), tBuMA (1.65 g) and PMDETA (0.012g) were dissolved in anisole (11 mL). Three freeze-pump-thaw cycles were performed and then Cu(I)Cl (0.007g) was added under positive Ar flow. The reaction mixture was sealed under Ar atmosphere before being heated to 45° C. After 1 hour, the reaction mixture was cooled down in liquid N_2, opened to air and precipitated into hexanes twice. Obtained white solid was dried under vacuum for 24 hours. Yield: 31% (0.6g). DP (tBuMA) = 65 as determined by ^{1}H NMR. Resulted polymer (0.5 g), was dissolved in 12 mL of dioxane and 0.45 mL of concentrated HCl was added to the polymer solution. Reaction mixture was stirred for 20h at 90° C, upon completion, reaction mixture was cooled down and precipitated into hexanes. Yield: 56% (0.28g).^{1}H NMR (400 MHz, CD_3OD, δ in ppm) = 7.5-6.16 (br. m., 178 H), 3.2-1.7 2.63 (br. m., 193H), 1.70-0.5 (br. m., 230H). DLS (water): Mw = 294 kDa (1.31).

Synthesis of DVB-PS-PMAA$_{50\%}$/PEGMA$_{50\%}$. ATRP-macroinitiator nanogel star polymer (2.0 g, Mn arm = 3.2 kDa, 31 arms), tBuMA (8.0 g), PEGMA (16.9 g) and PMDETA (0.10g) were dissolved in anisole (70 mL). Three freeze-pump-thaw cycles were performed and then Cu(I)Cl (0.06g) was added under positive Ar flow. The reaction mixture was sealed under Ar atmosphere before being heated to 45° C. After 90 min, the reaction mixture was cooled down in liquid N_2, opened to air and precipitated into hexanes twice. Obtained white gooey solid was dried under vacuum for 24 hours. Yield: 23% (6.1g). Resulted polymer, 5 g was dissolved in 120 mL of dioxane and 4.5 mL of concentrated HCl was added to the polymer solution. Reaction mixture was stirred for 20h at 90° C, upon completion, the reaction mixture was cooled down and precipitated into hexanes. Yield: 63%% (3.15g). ^{1}H NMR (400 MHz, $CDCl_3$, δ) = 7.25-6.25 (br. m, 153 H), 4.32-3.97 (br. s, 44H), 3.57 (s, 46H), 3.77-3.62 (br. m, 305H), 3.4 (s, 67H), 2.10-1.75 (br. s, 113H), 1.7 (s, 115H), 1.43 (s, 308H), 1.2-0.6 (br. m, 171H). DLS (THF): Mw = 285 kDa (1.25), DP (PEGMA) = 22, DP (PMAA) = 23 based on ^{1}H NMR

Synthesis of DVB-PS-PDMAEMA$_{50\%}$/PEGMA$_{50\%}$. ATRP-macroinitiator nanogel star polymer (2.0 g, Mn arm = 2.8 kDa, 35 arms), DMAEMA (8.5g), PEGMA (17.1g) and PMDETA (0.12g) were dissolved in anisole (65 mL). Three freeze-pump-thaw cycles were performed and then Cu(I)Cl (0.07g) was added under positive Ar flow. The reaction mixture was sealed under Ar atmosphere before being heated to 45^{o} C. After 90 min, the reaction mixture was cooled down in liquid N_2, opened to air and precipitated into hexanes twice. Obtained white gooey solid was dried under vacuum for 24 hours. Yield: 24% (6.7 g). ^{1}H NMR (400 MHz, $CDCl_3$, δ) = 7.25-6.25 (br. m, 135 H), 4.11 (br. s, 63H), 3.80-3.62(br. s, 50H), 3.62-3.55 (br. s, 15H), 3.4 (s, 34H), 2.85-2.55 (br. s, 23H), 2.55-2.30 (br. s, 61H), 2.3-1.7 (br. m, 76H), 1.7-1.2 (br. m, 68H), 1.15-0.68 (br. m, 56H). DLS (THF): Mw = 300 kDa (1.22), DP (PEGMA) = 11, DP (DMAEMA) = 19 based on ^{1}H NMR

SAXS Experiments: In this work, X= and/or Y= PEGMA, PMAA (acidic), or PDMAEMA (basic) (see insets of Figures 1-4 and further details are given in Table 1). We have quantified the size and shape as a function of pH using small angle X-ray scattering (SAXS) of the following series of star nanoparticles which differ in their outer block chemical composition: DVB-PS-PEGMA, DVB-PS-PDMAEMA, DVB-PS-PMAA and statistical compositions of basic and acidic units, DVB-PS-PDMAEMA$_{50\%}$/PEGMA$_{50\%}$ and DVB-PS-PMAA$_{50\%}$/ PEGMA$_{50\%}$.

The SAXS experiments were conducted on the SIBYLS beamline (12.3.1) at the Advanced Light Source synchrotron[20,21]. For each SAXS experiment, samples were prepared in a standard 25 μl 96-well plate to examine each star polymer as a function of pH at two or more concentrations (somewhere between 1.0 mg/ml and 5.0 mg/ml). Incident X-rays were tuned to a wavelength (λ) of 1.03 Å at a sample-to-detector distance of 1.5 m, resulting in scattering data collected continuously with the momentum transfer, $Q = 4\pi\sin(\theta/2)/\lambda$ (where 2θ is the scattering angle), over a range from 0.007 to 0.324 Å^{-1} with exposures of 0.5, 1, 2 and 6 seconds. All experiments were performed at 20°C. All data were scaled and buffer subtracted, and then averaged with the ScÅtter 2.0 package. Radii of gyration (R_G) were evaluated using the Guinier approximation, and analytical form factors were fit using SasView 3.1.1.[22]

SAXS Theory: The scattering intensity of a monodisperse system of particles can be described as follows:

$$I(Q) = NP(Q)S(Q) \quad (1)$$

Where I(Q) is the experimental scattering intensity, N is the number of particles, P(Q) is the single particle scattering function, also known as the form factor, and S(Q) is the interparticle scattering function that accounts for interactions between particles. In this work we are primarily interested in the shape and

size of the individual star polymers as a function of pH given potential applications such as drug delivery; hence we are interested in P(Q) and not S(Q). Therefore to ascertain the presence of intermolecular correlations (such as aggregation or particle repulsions) for each member of the pH series for each star polymer, we scaled the intensity of the different concentrations to each other. The intensity profiles matched exactly for DVB-PS-PEGMA, DVB-PS-PDMAEMA, DVB-PS-PDMAEMA$_{50\%}$/PEGMA$_{50\%}$ and DVB-PS-PMAA$_{50\%}$/ PEGMA$_{50\%}$, so that for these star polymers we can assume that S(Q)=1 and that any intensity features arise from the form factor of the individual particles. However the intensities for the DVB-PS-PMAA star polymer at different concentrations, for all pH values, did not scale to each other, indicating that there are interparticle correlations. Therefore for the 100% acid star polymer series we extrapolated the intensity of each Q-value to zero concentration in order to generate intensity curves in which S(Q)=1 is a good approximation, thus allowing us to fit the star polymer form factor and to perform a Guinier analysis for a single DVB-PS-PMAA star polymer.

The initial model-free analysis of the SAXS intensity data for the DVB-PS-PX$_n$PY$_m$ star polymers using a Kratky plot of $I*Q^{5/3}$ vs. Q is presented in Figure 1. With the exception of the 100% acidic star polymer, all of the remaining star polymers at any pH value exhibit an overall globular shape, i.e. a peak at low Q (Figure 1a-d). Since the intensity does not decay after the first maximum, it supports a structural model of swollen chain statistics consistent with polymeric arms in a good solvent. It is interesting to note that the Kratky plot for the DVB-PS-PMAA is markedly different from the others, with no intensity maximum. Given the initial model-free analysis, we sought to find analytical functions that fit the SAXS data for the different DVB-PS-PX$_n$PY$_m$ star polymers to gain more information about the size and structure in their response to changes in pH. The SAXS data did not fit several basic shapes such as uniform spheres, cylinders and ellipses, while the ‘block copolymer micelle’ model was a slightly better fit than those shapes, but still could not adequately fit all regions of the plot. However, we were able to identify three particle scattering functions, each of which performs well depending on pH or polymer series considered: the Dozier star polymer model[23,24], the poly-disperse core shell (PCS) model[25,26] or the Gaussian coil excluded volume (GCEV) model[27],

The star polymer form factor due to Dozier and coworkers[23,24] is based on the Cotton and Daoud “blob” polymer model[28] that describes the star polymer as a succession of concentric rings of “blobs” of size, ξ, and within each blob, the polymer chain is described as a random coil. The resulting Dozier form factor:

$$P(Q, I_0, R_G, \alpha, \nu, \xi) = P_0 \exp\left(\frac{-Q^2 R_G^2}{3}\right) + \frac{4\pi\alpha}{Q\xi}\Gamma(\mu)\frac{\sin\left(\mu \arctan(Q\xi)\right)}{\left(1+Q^2\xi^2\right)^{\mu/2}} \quad (1)$$

was developed to fit to two separate Q-regions of scattering. The first term accounts for the overall size and shape of the star particle and determines its R_G, where P_0 is an intensity scale parameter that adjusts the fit at small Q. The second term accounts for the scattering at large Q, and corresponds to the Fourier transform of the structural correlations within the star polymer arms, where both α (an intensity scale factor) and ξ are used to adjust the fit to the data at large Q. The intensity at large Q should decay like $e^{-\mu-1}$, where μ = (1/ν) – 1, ν is the Flory exponent, and Γ(μ) is the gamma function. Given the nature of the star polymers investigated here, ν was fixed at a value of 2/3 to represent the polymer arms as chains in a good solvent.

The PCS model[25,26], in contrast to the Dozier model, does not take into account the structural correlations in the star polymers explicitly, but instead considers the polymer as a core-shell structure, in which multiple concentric shells of different densities are considered. We also took into account the size distribution of the scattering particles by modeling the intensity scattered from a poly-disperse system:

$$I_{PCS}(Q) = I_o \int_0^\infty D_n(R)\, P(Q,R)\, dR \quad (2)$$

where I_0 is an intensity scaling factor and $D_n(R)$ is a Gaussian distribution

$$D_n(R) = \exp\left[-\left(\frac{\left(R - \langle R\rangle^2\right)}{2\sigma^2}\right)\right] \quad (3)$$

where <R> is the average radius that accounts for the poly-dispersity in size (not mass), δ=σ/<R>. The form factor for the core shell model is:

$$P(Q,R) = \left[\frac{4\pi R_C^3}{3}(\rho_C - \rho_{S1})\,\Phi(QR_C) + \frac{4\pi R_{S1}^3}{3}(\rho_{S1} - \rho_{S2})\,\Phi(QR_{S1}) + \frac{4\pi R_{S2}^3}{3}(\rho_{S2} - \rho_{solv})\,\Phi(QR_{S2})\right]^2 \quad (4a)$$

where R_C is the radius of the core, R_{Si} the radius of the ith shell from the core, ρ_C is the scattering length density of the core, ρ_{Si} is the scattering length density of the ith shell from the core, ρ_{solv} is the scattering length density of the solvent, and Φ, the normalized amplitude scattered by a sphere, is computed as follows:

$$\Phi(QR) = 3\left[\frac{\sin(QR) - QR\cos(QR)}{QR^3}\right] \tag{4b}$$

We used 9.4*10^{-6} Å^{-2} for the scattering length density (SLD) of H_2O when fitting the data with the PCS model. The NIST calculator (https://www.ncnr.nist.gov/resources/sldcalc.html) was used to obtain initial estimates of the SLD for each polymer core or shell region.

Finally, the GCEV model for the scattering of an isolated ideal Gaussian coil in solution[29] involves a semi-analytical functional form:

$$P(Q, R_G, z) = \frac{1}{z\,U^{1/2z}}\gamma\left(\frac{1}{2z}, U\right) - \frac{1}{z\,U^{1/z}}\gamma\left(\frac{1}{z}, U\right) \tag{5a}$$

where z is the excluded volume parameter, γ(x, U) is the incomplete gamma function:

$$\gamma(x, U) = \int_0^U dt\,\exp(-t)\,t^{x-1} \tag{5b}$$

and the variable U is a function of Q and the fit parameters z and R_G:

$$U(Q, R_G, z) = \frac{Q^2 R_G^2 (2z+1)(2z+2)}{6} \tag{5c}$$

For all of the series studied, with the exception of DVB-PS-PMAA, there is an evident transition at a particular pH that depends on the absence or presence of a peak in the data at Q ~ 0.04 – 0.06 Å^{-1}, which corresponds to a better fit obtained with a Dozier or PCS model, respectively. By contrast, the DVB-PS-PMAA series was instead fit solely by the GCEV model since no structural transition is evident, and furthermore the intensity is dominated by repulsive intermolecular correlations.

RESULTS

Figure 2 shows the trend in the SAXS intensity for the DVB-PS-PEGMA star polymer when titrated over a large pH range; the inset shows the trend in R_G as a function of pH based on the fits to the SAXS data using the analytical Dozier model (Table S1). Although PEGMA is well known to be temperature sensitive, it is expected that it will be unresponsive to any pH changes, and this is born out in Figure 2 inset that shows that the R_G remains constant throughout the titration.

It is interesting to note that the DVB-PS-PEGMA star is well-fit by the Dozier model of a swelled star polymer – a model which is better able to resolve the smaller scale structure in the higher Q regions manifested as “blob” scattering from individual arm chains that are more solvent exposed. This property

of DVB-PS-PEGMA is well appreciated, and we have shown previously[30] using molecular dynamics on a related PEG star polymer, that the thermodynamic origins of a structural transition as temperature increases is consistent with entropy-driven dehydration such that below the lower critical solution temperature the PEG arms act like a Gaussian random coil. Thus the DVB-PS-PEGMA star polymer serves as a reference point for introduction of monomer units that are in fact sensitive to pH.

Figure 3a shows the trend in the SAXS intensity when titrated over a pH range from 3.18-9.26 for the basic star polymer in which 100% of the PEGMA units are replaced by PDMAEMA; the inset shows the trend in R_G as a function of pH for DVB-PS-PDMAEMA based on the fits to the SAXS data using the analytical models (Table S2). It is seen that there is a relatively sharp transition in the size of the basic star polymer as pH decreases near pH~5.5-6.0, in line with estimates of the apparent pKa shown in the titration curve in Figure 3b. While the pKa,app of the DMAEMA monomer is ~8.4, previous studies have indicated a greater ease in deprotonation for linear forms of the PDMAEMA polymer relative to the DMAEMA monomer due to electrostatic repulsions between charged groups along the chain that shifts the pKa,app to a smaller value of ~7.0-7.2[31,32]. This pKa,app shifts to even smaller values for a reported PDMAEMA star polymer (5.8-6.3)[18] due to greater electrostatic repulsion between the arms imposed by the star polymer architecture.

However, Figure 4a shows that random replacement of only half of the PEGMA monomers with DMAEMA results in a sharp structural transition (as measured by R_G values) at even lower pH than measured for the 100% DMAEMA substituted polymers. This is supported by two independent pieces of evidence. First is that the intensity is well fit by the PCS form factor above pH~4.5, while below this pH value the polymer swells as evidenced by the need to reproduce the high-Q intensity data with the Dozier form factor (Table S3). In addition, based on the main equivalence point in Figure 4b, we estimate the pKa,app ~ 4.5. Therefore any available hydronium ions merely contribute to lowering the pH of the solution, until a pH of 4.5 when the PDMEAMA now becomes protonated and causes significant swelling of the star polymer. This would be consistent with the study conducted on the linear form of the random PDMAEMA-PEGMA co-polymer that showed an increase in the LCST as the proportion of PEGMA increased at any pH, which disappeared entirely at a pH=4 for the linear $PDMAEMA_{50\%}/PEGMA_{50\%}$ polymer[33].

The 50% acidic star polymer, DVB-PS-$PMAA_{50\%}/PEGMA_{50\%}$, shows the opposite trend in the SAXS intensity profile and fits (Figure 5a and Table S4) as a function of pH relative to any of the basic series of

polymers when titrated over a pH range from 5.18-9.6. We would expect the acidic star polymer to become negatively charged at pH values above the usual estimate of the pKa,app ~4 for polymethacrylate acid, but the introduction of PEGMA clearly has modulated this response so that the conjugate base form of PMAA is not realized until much larger pH values above ~7.5; this again is supported by the titration curve in Figure 5b. To put this remarkable result into perspective, for the linear polymer architecture the hydrogen bonding between the protonated form of PMAA with PEG results in weakly stable interpolymer complexes[34,35], that dissemble just above the usual pKa,app for PMAA. When PMAA and PEG are put together as a diblock linear polymer the intramolecular interactions stabilize the protonated form to slightly larger pH values up to ~5.5.[36] However, when PMAA and PEGMA are placed onto a star polymer architecture, the effective increase in functional group concentration contributes to multiple hydrogen-bonding interactions that act to resist deprotonation of the PMAA over a much larger pH range, with a structural transition to the extended form delayed until well into the high pH values.

By contrast, the DVB-PS-PMAA star polymer shows no distinct structural transition as a function of pH in either the SAXS intensity (Figure 6a) or fit to the GCEV model (Table S5). There is overall no clear trend in the R_G of the polymer as a function of increasing pH, which is partly due to numerical noise arising from the extrapolation of each Q point to zero concentration to remove the stronger repulsive intermolecular correlations that dominate the SAXS intensity. Nonetheless, the overall size of the 100% acidic star polymer is greatly expanded at all pH values relative to the 50% acidic star polymer, and further supports the conclusion that PEGMA modulates the structural transition by complexation with PMAA.

DISCUSSION AND CONCLUSIONS

While the DVB-PS-PEGMA and DVB-PS-PMAA polymers showed no structural transition as a function of pH, we found that a pH sensitive change was observed in the SAXS intensity that indicate the collapse or expansion of the polymeric arms for DVB-PS-PDMAEMA, DVB-PS-$PMAA_{50\%}$/$PEGMA_{50\%}$, and DVB-PS-$PDMAEMA_{50\%}$/$PEGMA_{50\%}$. What is surprising is that the structural transition is triggered at pH values that can be quite different when compared to the pKa of the monomer unit or pKa of the linear forms of highly similar polymer compositions or even star architectures.

One interesting aspect of the nanogel stars investigated here relative to these other stars of traditional core structure is that the presence of a hydrophobic block (PS) connected to the DVB core results in an expanded hydrophobic region, presumably with a larger surface area from which the corona arms extend.

The increased surface area of the core should lead to less interaction between the arms than would be encountered if instead they would be connected at a point as is the case with the tight cross-linked core PDMAEMA star polymer[18]. Therefore, it is reasonable to expect that the apparent pKa value for the nanogel core DVB-PS-PDMAEMA star polymer should be somewhere in between the values reported for linear PDMAEMA (7.0-7.2)[31,32] and the small core PDMAEMA star polymer (5.8-6.3)[18]. The fact that we measure the structural transition to larger R_G between pH~6.0-7.0, illustrates the interesting result that one can dial in pH-induced structural transitions through properties of the star polymer core.

The shift in apparent pKa for the PDMAEMA-PEGMA is particularly unexpected. In principle, the dilution of the amine in the polymer by the PEGMA unit should have the effect of slightly increasing the pKa,app which means that the size change should occur at higher pH, which it clearly does not. If there was a stabilizing complexation between the protonated amine and the PEG, this also should have the effect of raising the apparent pKa,app relative to the homopolymer; this also doesn't seem to happen since the size transition occurs below pH 5. There is no direct evidence of complexation reported between PEGMA and DMAEMA units at higher pHs which would result in a decrease in the apparent basicity and a shift in the pH curve. There is literature evidence of complexation between quaternary amine functionality and PEG units[37] and hence presumably also between protonated amino substituents, but this would result in an increase of the apparent basicity of the dimethylamino substituted polymer, and again a curve shift to more basic pHs which is not observed by the SAXS dimensional changes nor the titration curves. Instead we can only attribute our observations to an indirect effect based on the preference of the highly hydrophilic PEGMA for the basic form of PDMAEMA since both can form good hydrogen-bonding interactions with water.

The direct stabilization of the neutral form of PMAA by PEGMA up to very high pH values is reminiscent of the large shifts in pKa observed for amino acids such as histidine (pKa~6), whose protonated acidic form is stabilized by ion-dipole interactions with aspartic acid, thereby shifting histidine’s pKa to ~12, to create a so-called his-asp dyad that can serve as a catalytic base for many enzymes. Similarly, this has been observed previously in studies that report the contraction of a PMAA membrane as a function of increasing PEG content[38]; as the PEG content increased, the PMAA membrane contracted more extensively over a shorter period of time. For the 100% acidic series on the other hand, there is no notable collapse, only an increase in repulsion between star polymers as a function of increasing pH, emphasizing that compositional changes in PEGMA fraction can further fine tune the desired pH at which the structural transition occurs.

It should be noted that these experiments were performed at 20°C, whereas for the targeted application of these systems, the polymers will be at physiological temperatures of ~ 37°C. The coupling of temperature and pH may have a complex effect on the structural transitions and the pKa's reported here. The dual sensitivity of systems to temperature and pH has been studied before[39,40], in which some systems gave independent responses to the two system parameters[41], while others show an interplay between the two stimuli[42]. However, while both the linear forms of PDMAEMA and PEGMA are known to have lower critical solution temperatures (LCST) of 50°C[43] for the former and in the range of 80-90°C for the latter (dependent on PEG side-chain length)[44], we expect the effect of temperature will be small given that physiological temperature is much lower than the LCST. Nonetheless, the nature of the polymer architecture and the length of polymer chains could give rise to unanticipated interplay between temperature and pH sensitivity, and should be considered for future studies.

In summary, we find that properties of the star polymer core and/or arm chemistry can be used to induce a sharp structural transition over a narrow range of pH, an interpretation that is supported by the corresponding titration curves of all star polymers investigated. While the effect is often easily understood by complexation between the monomer components at lower (higher) pHs and an increase (decrease) in the apparent pKa, this has not been demonstrated previously in a star polymer.

ACKNOWLEDGEMENTS

This work was supported by the Director, Office of Science, Office of Basic Energy Sciences, of the U.S. Department of Energy under Contract No. DE-AC02-05CH11231. LF was supported by the National Science Foundation Graduate Research Fellowship under Grant No. DGE 1106400 and AD was supported by the Amgen scholars program. The SAXS work was conducted at the Advanced Light Source (ALS), a national user facility operated by Law-rence Berkeley National Laboratory on behalf of the Department of Energy, Office of Basic Energy Sciences, of the U.S. DOE under Contract No. DE-AC02-05CH11231, as well as through the Integrated Diffraction Analysis Technologies (IDAT) program, supported by DOE Office of Biological and Environmental Research, with additional support comes from the National Institute of Health project MINOS (R01GM105404). This work benefited from SasView software, originally developed by the DANSE project under NSF award DMR-0520547.

REFERENCESX[1]Tao Wang, Gerard G. M. D'Souza, Deepa Bedi, Olusegun A. Fagbohun, L. Prasanna Potturi, Brigitte Papahadjopoulos-Sternberg, Valery A. Petrenko, and Vladimir P. Torchilin, *Nanomedicine* **5** (4), 563 (2010).
[2]Chie Kojima, Celeste Regino, Yasuhito Umeda, Hisataka Kobayashi, and Kenji Kono, *Int. J. Pharm.* **383** (1), 293 (2010).
[3]R. Gref, Y. Minamitake, M.T. Peracchia, V. Trubetskoy, V. Torchilin, and R. Langer, *Science* **263**, 1600 (1994).
[4]Sidi A. Bencherif, Haifeng Gao, Abiraman Srinivasan, Daniel J. Siegwart, Jeffrey O. Hollinger, Newell R. Washburn, and Krzysztof Matyjaszewski, *Biomacromolecules* **10** (7), 1795 (2009).
[5]Ken-Ichi Fukukawa, Raffaella Rossin, Aviv Hagooly, Eric D. Pressly, Jasmine N. Hunt, Benjamin W. Messmore, Karen L. Wooley, Michael J. Welch, and Craig J. Hawker, *Biomacromolecules* **9** (4), 1329 (2008).
[6]Theoni K Georgiou, Maria Vamvakaki, Leonidas A Phylactou, and Costas S Patrickios, *Biomacromolecules* **6**, 2990 (2005).
[7]D. Schmaljohann, *Adv Drug Deliv Rev* **58** (15), 1655 (2006).
[8]H. Almeida, M. H. Amaral, and P. Lobão, *Journal of Applied Pharmaceutical Science* **2** (6), 1 (2012).
[9]Gianfranco Pasut and Francesco M. Veronese, *Adv. Drug Del. Rev.* **61**, 1177 (2009).
[10]Michelle Longmire, Peter L. Choyke, and Hisataka Kobayashi, *Nanomedicine* **3** (5), 703 (2008).
[11]J. M. Harris and R. B. Chess, *Nat. Rev. Drug. Discov.* **2003** (2), 214 (2003).
[12]E. Fleige, M. A. Quadir, and R. Haag, *Adv Drug Deliv Rev* **64** (9), 866 (2012).
[13]Anton Blencowe, Jing Fung Tan, Tor Kit Goh, and Greg G. Qiao, *Polymer* **50** (1), 5 (2009).
[14]Jean Georges Zilliox, Paul Rempp, and Jacques Parrod, *J. Polym. Sci. Polym. Symp.* **22** (Pt. 1), 145 (1968).
[15]J. M. Ren, Q. Fu, A. Blencowe, and G. G. Qiao, *ACS Macro. Lett.* **1**, 681 (2012).
[16]E. A. Appel, V. Y. Lee, T. T. Nguyen, M. McNeil, F. Nederberg, J. L. Hedrick, W. C. Swope, J. E. Rice, R. D. Miller, and J. Sly, *Chemical communications* **48** (49), 6163 (2012).
[17]Nahrain E. Kamber, Wonhee Jeong, Robert M. Waymouth, Russell C. Pratt, Bas G. G. Lohmeijer, and James L. Hedrick, *Chem. Rev.* **107** (12), 5813 (2007).
[18]J. F. Tan, F. A. Plamper, M. Ruppel, A. Schmalz, O. Borisov, M. Ballauff, and A. H. E. Müller, *Macromolecules* **40** (23), 8361 (2007).
[19]V. Y. Lee, K. Havenstrite, M. Tjio, M. McNeil, H. M. Blau, R. D. Miller, and J. Sly, *Advanced materials* **23** (39), 4509 (2011).
[20]G. L. Hura, A. L. Menon, M. Hammel, R. P. Rambo, F. L. Poole, 2nd, S. E. Tsutakawa, F. E. Jenney, Jr., S. Classen, K. A. Frankel, R. C. Hopkins, S. J. Yang, J. W. Scott, B. D. Dillard, M. W. Adams, and J. A. Tainer, *Nat Methods* **6** (8), 606 (2009).
[21]S. Classen, G. L. Hura, J. M. Holton, R. P. Rambo, I. Rodic, P. J. McGuire, K. Dyer, M. Hammel, G. Meigs, K. A. Frankel, and J. A. Tainer, *J Appl Crystallogr* **46** (Pt 1), 1 (2013).
[22]http://www.sasview.org/, in *SasView* (http://www.sasview.org/, 2015).
[23]H. Benoit, *Journal of Polymer Science* **11** (5), 507 (1953).
[24]W. D. Dozier, J. S. Huang, and L. J. Fetters, *Macromolecules* **24** (10), 2810 (1991).
[25]S. R. Kline and E. W. Kaler, *J Colloid Interface Sci* **203** (2), 392 (1998).
[26]S. Ruthstein, A. M. Raitsimring, R. Bitton, V. Frydman, A. Godt, and D. Goldfarb, *Phys Chem Chem Phys* **11** (1), 148 (2009).
[27]B. Hammouda, *Advances in Polymer Science* **106**, 87 (1993).
[28]M. Daoud and J. P. Cotton, *J. Phys. (Paris)* **43**, 531 (1982).
[29]P. Debye, *Journal of Physical and Colloid Chemistry* **51** (1), 18 (1947).

[30]L. E. Felberg, D. H. Brookes, T. Head-Gordon, J. E. Rice, and W. C. Swope, *J Phys Chem B* **119** (3), 944 (2015).
[31]B.-S. Kim, H. Gao, A. A. Argun, K. Matyjaszewski, and P. T. Hammond, *Macromolecules* **42** (1), 368 (2009).
[32]H. Lee, S. H. Son, R. Sharma, and Y.-Y. Won, *J. Phys. Chem. B* **115** (5), 844 (2011).
[33]D. Fournier, R. Hoogenboom, H. M. L. Thijs, R. M. Paulus, and U. S. Schubert, *Macromolecules* **40**, 915 (2007).
[34]K. Abe, M. Koide, and E. Tsuchida, *Macromolecules* **10** (6), 1259 (1977).
[35]Y. Yokoyama and S. Yusa, *Polymer Journal* **45**, 985 (2013).
[36]S. Holappa, L. Kantonen, F. M. Winnik, and H. Tenhu, *Macromolecules* **37**, 7008 (2004).
[37]T. Andersson, M. Sumela, L. Khriachtchev, M. Räsänen, V. Aseyev, and H. Tenhu, *J. Polym. Sci. B Polym. Phys.* **46**, 547 (2008).
[38]Y. Osada, *Journal of Polymer Science Part C-Polymer Letters* **18** (4), 281 (1980).
[39]G. H. Jiang, X. K. Sun, Y. Z. Zhu, and Y. Wang, *Designed Monomers and Polymers* **14** (2), 167 (2011).
[40]L. Ma, R. Liu, J. Tan, D. Wang, X. Jin, H. Kang, M. Wu, and Y. Huang, *Langmuir* **26** (11), 8697 (2010).
[41]Soon Hong Yuk, Sun Hang Cho, and Sang Hoon Lee, *Macromolecules* **30** (22), 6856 (1997).
[42]X. Han, X. X. Zhang, H. F. Zhu, Q. Y. Yin, H. L. Liu, and Y. Hu, *Langmuir* **29** (4), 1024 (2013).
[43]S. H. Cho, M. S. Jhon, and S. H. Yuk, *European Polymer Journal* **35** (10), 1841 (1999).
[44]C. R. Becer, S. Hahn, M. W. M. Fijten, H. M. L. Thijs, R. Hoogenboom, and U. S. Schubert, *Journal of Polymer Science Part a-Polymer Chemistry* **46** (21), 7138 (2008).

Table 1. *Details of the nanogel star polymers.* The nanogel core is a cross-linked DVB core, and all star polymers have a common inner block of polystyrene. The star polymers differ in their outerblock hydrophilic chemistry, composed of either pure PEGMA, pure PDMAEMA, pure PMAA, or the 50-50 series which are statistical compositions of the PMAA acidic or PDMAEMA basic groups with PEGMA.

Star Polymer	**PEGMA**	**PDMAEMA**	**PMAA**	**PDMAEMA$_{50\%}$/ PEGMA$_{50\%}$**	**PMAA$_{50\%}$/ PEGMA$_{50\%}$**
Total Molecular Weight (kDa)	315	233	294	300	285
PS block weight (kDa)	2.8	3.3	3.7	2.8	3.2
PDI	1.37	1.27	1.31	1.22	1.25
Average arm number	35	32	29	35	27
	Hydrophilic Block				
Hydrophilic block weight (kDa)	6.1	4.7	5.6	6.0	8.9
PEGMA Weight Fraction (Number of monomers)	1.00 (21)	0.00	0.00	0.53 (11)	0.78 (18)
PMMA Weight Fraction (Number of monomers)	0.00	0.00	1.00 (65)	0.00	0.22 (23)
PDMAEMA Weight Fraction (Number of monomers)	0.00	1.00 (30)	0.00	0.47 (18)	0.00

FIGURE CAPTIONS

Figure 1. *The Kratky plot of $I*Q^{5/3}$ vs. Q for selected stars at four pH values for* (a) DVB-PS-PDMAEMA, (b) DVB-PS-PDMAEMA$_{50\%}$/PEGMA$_{50\%}$ (c) DVB-PS-PMA$_{50\%}$/PEGMA$_{50\%}$ (d) DVB-PS-PEGMA (e) DVB-PS-PMAA. Data are shifted by a multiplication factor for clarity.

Figure 2. *Measured scattering curves for DVB-PS-PEGMA series in water from pH 9.48 (top) to pH 2.76 (bottom).* Experimental data are shown by colored dots and are shifted by a multiplication factor for clarity. Black solid lines are fits to the Dozier model, with the parameters given in Table S1. A metric of the experimental error is given by max(Err(Q)/I(Q)). The insert depicts the measured Guinier R_G for the 100% PEGMA series as a function of pH. The DVB-PS-PEGMA star polymer is composed of a cross-linked DVB core (orange), with diblock arm chemistries comprised of an inner hydrophobic pol-ystyrene block (black with y = 33), and outer hydrophilic PEGMA region (blue with x=30).

Figure 3. *(a) Measured scattering curves for DVB-PS-PDMAEMA series in water from pH 9.26 (top) to pH 3.18 (bottom) and (b) corresponding titration curve for DVB-PS-PDMAEMA.* Black solid lines are fits to Dozier or PCS model, with the parameters given in Table S2. The arrow indicates the transition from the Dozier to PCS model fit with increasing pH. The insert depicts the measured Guinier R_G for the 100% Basic series as a function of pH. The outer hydrophilic block is PDMAEMA (blue with x=30); see Figure 1 caption for other details.

Figure 4. (*a) Measured scattering curves in water from pH 9.47 (top) to pH 2.80 (bottom) and (b) corresponding titration curve for DVB-PS-PDMAEMA50%/PEGMA50% series.* Black solid lines are fits to Dozier or PCS model, with the parameters given in Table S3. The arrow indicates the transition from the Dozier to PCS model fit with increasing pH. The insert depicts the measured Guinier R_G for the 50% basic series as a function of pH. The outer block is a random copolymer with PDMAEMA50%/PEGMA50% region (blue with x=30); see Figure 1 caption for other details.

Figure 5. *(a) Measured scattering curves from pH 9.85 (top) to pH 5.11 (bottom), and (b) corresponding titration curve for DVB-PS-PMAA50%/PEGMA50% series in water.* Black solid lines are fits to Dozier or PCS model, with the parameters given in Table S4. The arrow indicates the transition from the PCS to Dozier model fit with increasing pH. The insert depicts the measured Guinier R_G for the 50% Acidic series as a function of pH. The outer block is a random copolymer with PMAA50%/PEGMA50% region (blue with x=30); see Figure 1 caption for other details.

Figure 6. *(a) Measured scattering curves from pH 12.30 (top) to pH 2.91 (bottom), and (b) corresponding titration curve for DVB-PS-PMAA series in water.* Black solid lines are fits to the GCEV model, with the parameters given in Table S5. The insert depicts the measured Guinier R_G for the 100% acidic series as a function of pH. The outer block is PMAA (blue with x=30); see Figure 1 caption for other details.

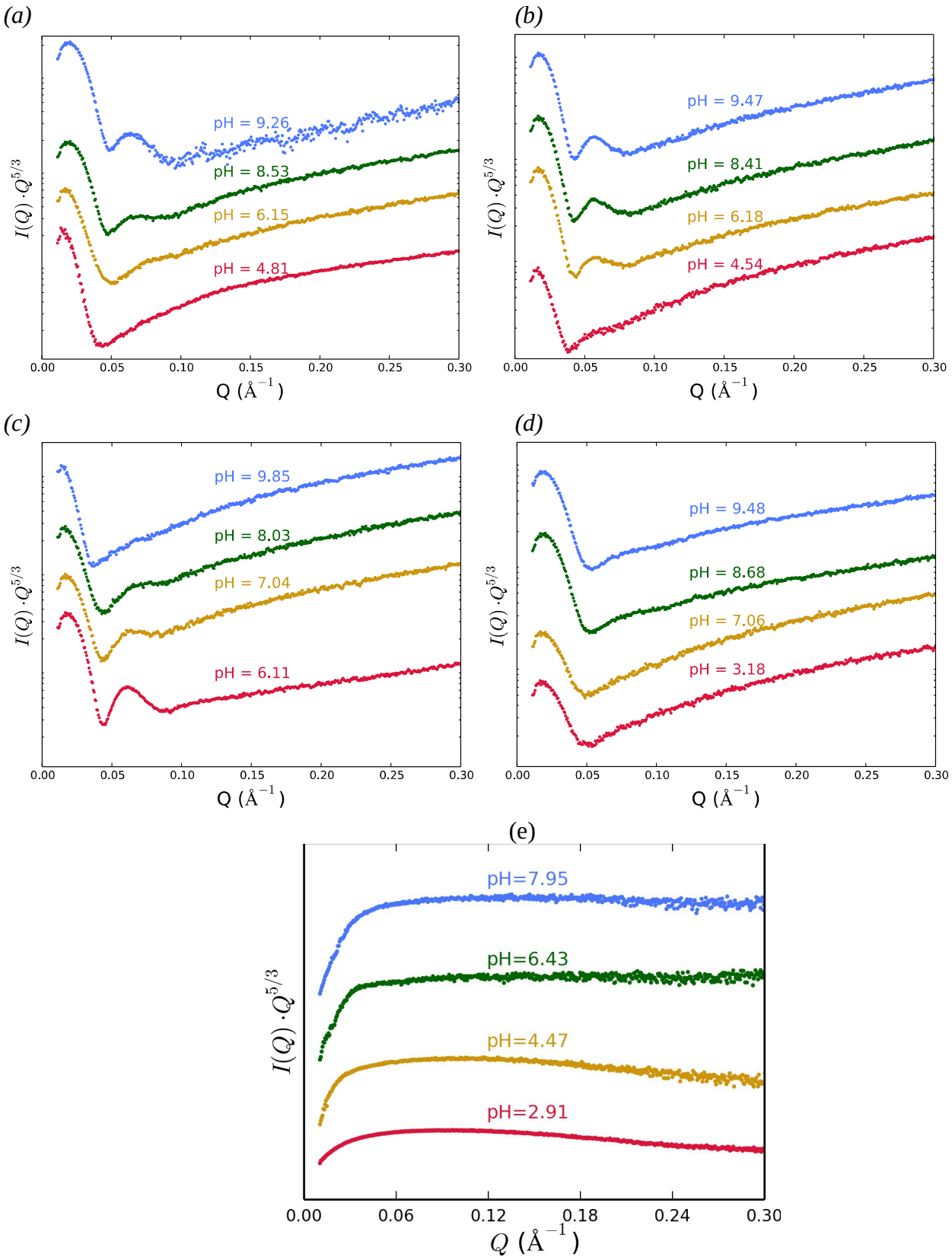

Figure 1. Felberg and co-workers

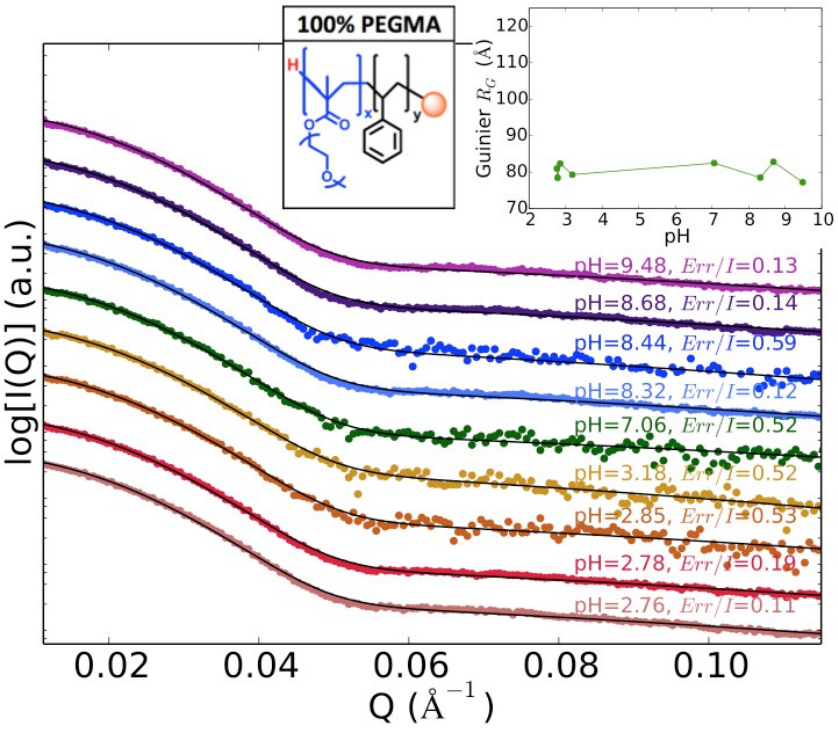

Figure 2. Felberg and co-workers

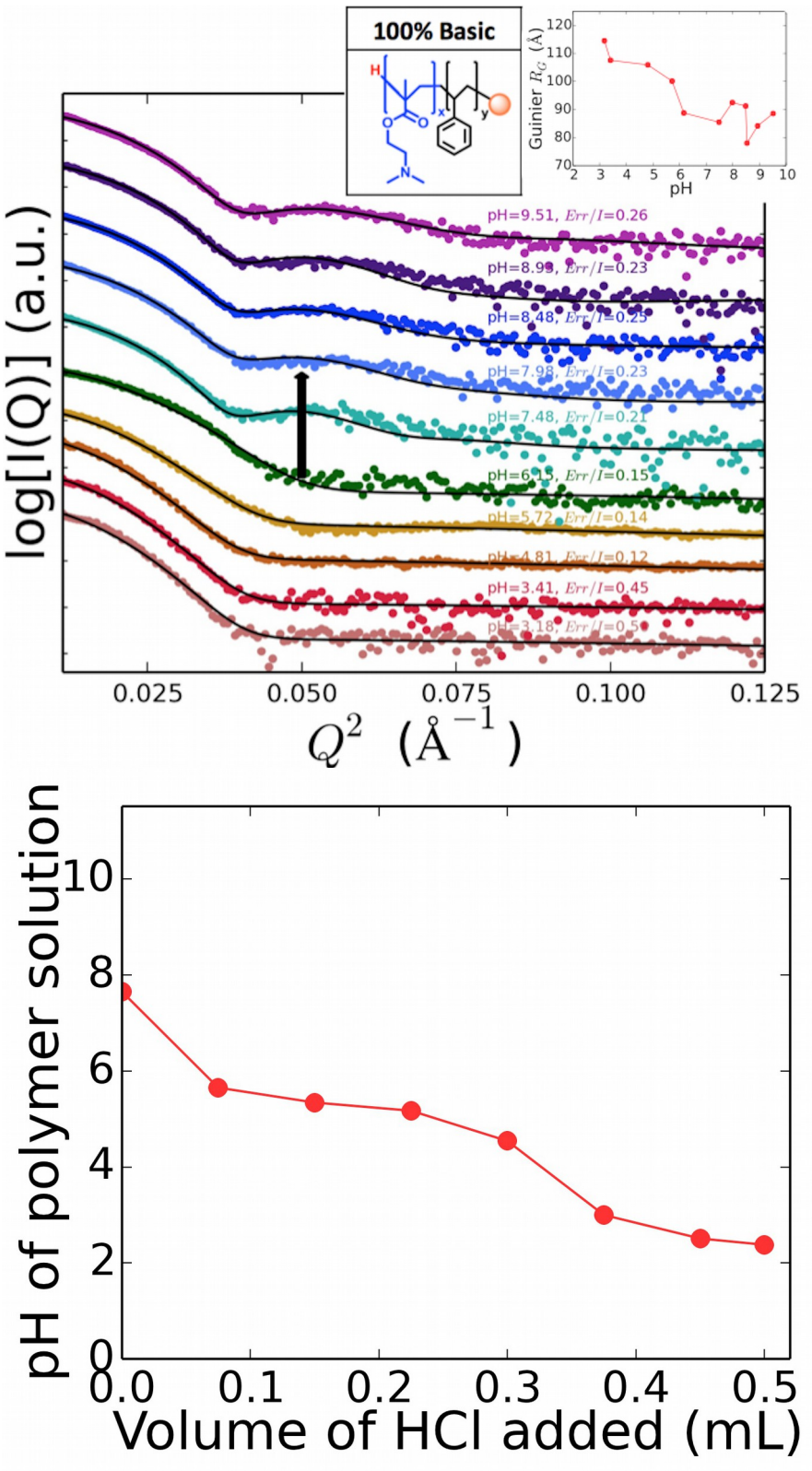

Figure 3. Felberg and co-workers

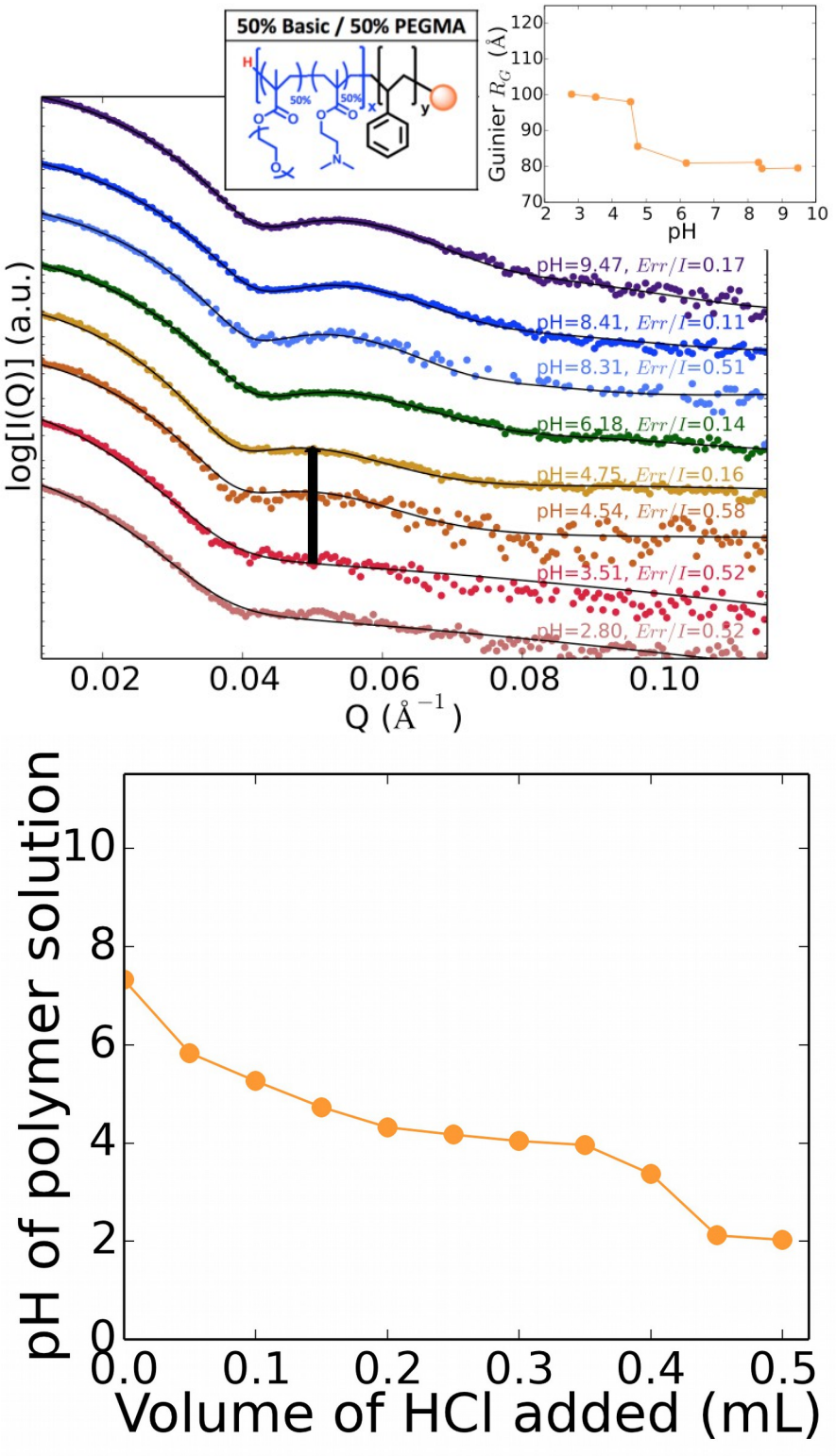

Figure 4. Felberg and co-workers

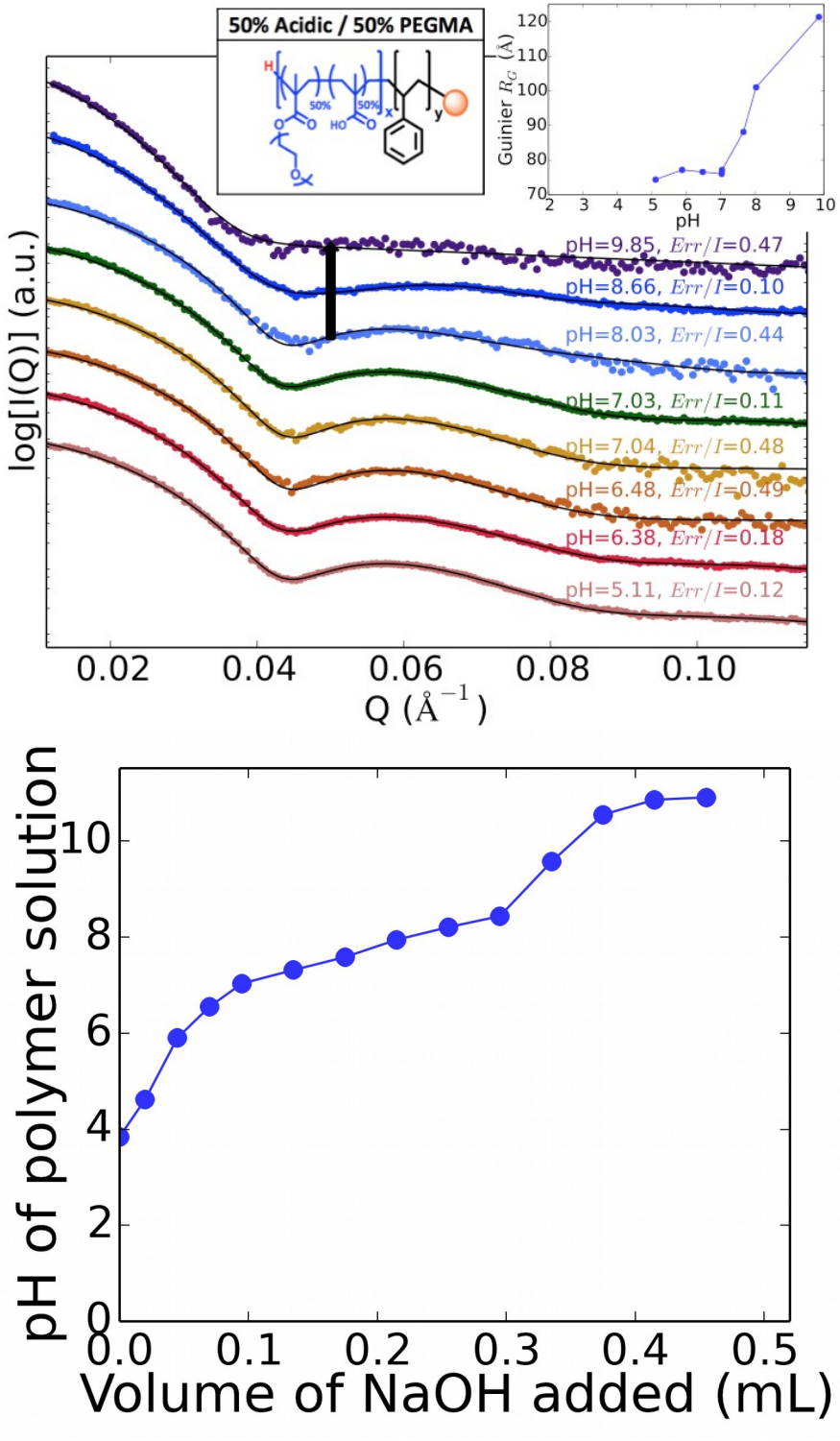

Figure 5. Felberg and co-workers

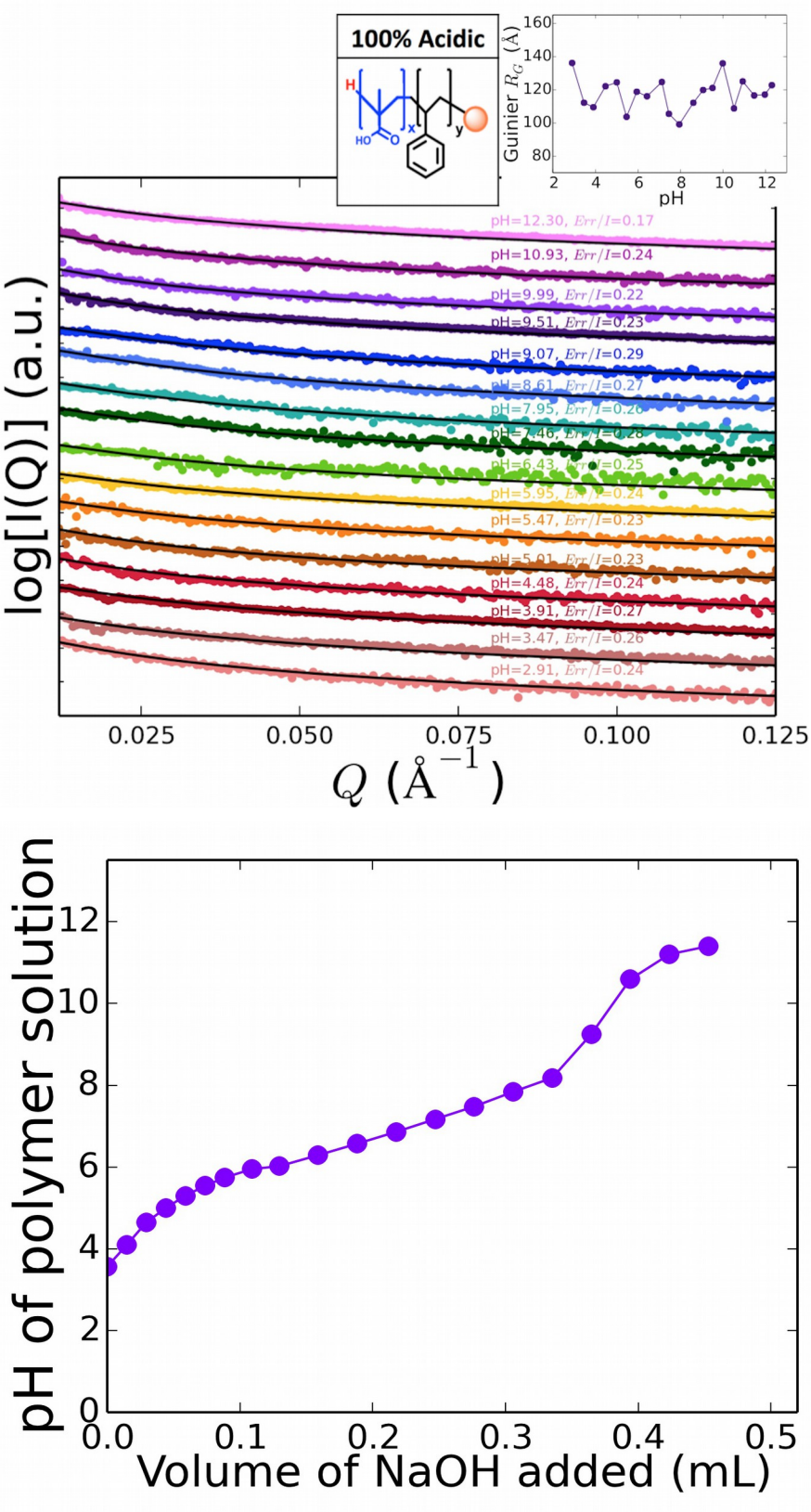

Figure 6. Felberg and co-workers